Journal of Applied Electrochemistry **31**: 997–1007, 2001.

Anodic behaviour of carbon materials in NaCl saturated $NaAlCl_4$ fused electrolyte at low temperatures: A cyclic voltammetric study

K.S. MOHANDAS[1]*, N. SANIL[1], M. NOEL[2] and P. RODRIGUEZ[1]
[1]*Materials Chemistry Division, Indira Gandhi Centre for Atomic Research, Kalpakkam, 603 102, India*
[2]*Central Electrochemical Research Institute, Karaikudi, 630 006, India*
*(*author for correspondence, fax: +91 4114 80065, e-mail: ksmd@igcar.ernet.in)*

Received 13 August 2000; accepted in revised form 27 March 2001

Key words: adsorption/desorption, chlorine, chloroaluminate, electrolysis, graphite, intercalation/deintercalation

Abstract

The anodic behaviour of compacted graphite, graphite powder, glassy carbon and reticulated vitreous carbon electrodes in basic sodium chloroaluminate melt in the temperature range 428–573 K was studied using cyclic voltammetry. Chlorine evolution (>+2.1 V vs Al) alone was the predominant reaction on the compact glassy carbon and fresh RVC electrodes. On compacted graphite, chlorine-assisted chloroaluminate intercalation was found to be a competitive process to the chlorine evolution. At high sweep rates, intercalation/deintercalation near the graphite lattice edges occur faster than chlorine evolution. Subsequent intercalation, however, is a slow process. Chlorine evolution predominates at higher temperatures and at higher anodic potentials. On graphite powders, a more reversible free radical chlorine adsorption/desorption process also occurs in the potential region below chlorine evolution. The process occurs at the grain boundaries, edges and defects of the graphite powder material. Intercalation/deintercalation processes are mainly responsible for the disintegration of graphitic materials in low-temperature chloroaluminate melts. Repeated intercalation/deintercalation cycles result in the irreversible transformation of the electrode surface and electrode characteristics. The surface area of the electrode is increased substantially on cycling. Electrode materials and operating conditions suitable for chlorine generation, intercalation/deintercalation and chlorine adsorption/desorption and power sources based on these processes are identified in this work.

1. Introduction

Graphite is considered as the anode of choice in the low-temperature sodium production process, where sodium tetrachloroaluminate ($NaAlCl_4$) is electrolysed via sodium ion conducting β-alumina at about 523 K. The patent [1] as well as some other reports [2] suggest that the graphite anode is inert in the basic chloroaluminate melt. However, the graphite anodes used in our studies disintegrated during electrolysis [3]. Wendt et al. [4] made a similar observation in acidic chloroaluminate and attributed this to the formation of graphite intercalation compounds (GIC) involving aluminium chloride and chlorine. Holleck [5] also reported that graphite anodes disintegrated in chlorine containing chloroaluminate melt. However, generally carbon anodes are reported [6] as inert in molten chloroaluminate. Wendt et al. [7] reported that the corrosive degradation of technical carbons, especially at elevated temperatures (above 773 K) is due to the formation of perchlorinated compounds like CCl_4, C_2Cl_4 etc. However, the results are based on the gas phase reaction of chlorine with carbon. It is possible that such reactions may contribute to the anodic corrosion of graphite in low-temperature (<573 K) electrolysis of molten chloroaluminate as well, although this is not confirmed in the literature.

Our examination of the reacted graphite anode in the sodium production cell had shown that substantial quantity of chlorine was reversibly trapped in the reacted graphite (GIC) and it can be used as a positive electrode for a sodium–chlorine or aluminium–chlorine secondary battery. So, it becomes apparent that the graphite can either be used as a stable chlorine-evolving anode or as a secondary chlorine storage medium (cathode) in chloroaluminate melt. It was felt that the conflicting reports on the stability of carbon electrodes cited above are related to these mutually exclusive properties of the electrode and their dependence on the type of carbon materials, employed under different experimental conditions. We have carried out electrochemical studies by using cyclic voltammetric (CV) and galvanostatic techniques on different types of carbon material to understand some of these aspects [8]. The results of the CV studies are reported in this paper.

The preliminary cyclic voltammetric experiments on compacted graphite (nonporous graphite material),

graphite foil (porous graphite), graphite powder (high surface area graphite), glassy carbon (compact vitreous carbon) and reticulated vitreous carbon or RVC (porous vitreous carbon) have indicated that three processes namely; chlorine evolution, chlorine gas induced chloroaluminate intercalation and loosely held chlorine adsorption on the active carbon sites take place on different types of carbon material. The electrode stability, exfoliation and deterioration depend on the level of graphitization, the particle size and porosity of the carbon materials. In addition to the type of electrode material, the effect of anodic potential limit, time (sweep rate), temperature and memory effects of prior polarization on these three competitive processes are also outlined in the paper.

2. Experimental details

2.1. *Electrodes*

Four different types of carbon material were used as the working electrodes in the CV studies. These are (i) compact graphite (rod, 6 mm dia., 99.9995%, Ultra Carbon, USA), (ii) graphite foil (1.5 mm thick, Graphite India, India), (iii) graphite powder (average size 6 μm, colloidal graphite, Graphite India, India), (iv) glassy carbon (rod, 2 mm dia., CY-2500, NIIGRAFIT, USSR) and (v) RVC (3 mm thick, RVC-1000, porosity 90%, Le Carbone Lorraine).

Fabrication details of the different electrodes are given in Figure 1(a), (b) and (c). The construction of the graphite rod and GC electrodes was similar. Both electrodes were provided with tight Teflon sleeves, so that a known length (area) was exposed in the molten electrolyte. The exposed area was either 0.5 cm^2 or 2 cm^2 for the graphite rod and 0.03 cm^2 for the GC electrode. The graphite powder (25 mg) and foil (8 mm dia. disc) electrodes were contained in a Teflon cup, similar in construction to that used by Maximovitch et al. [9]. A molybdenum foil shaped to 8 mm diameter disc with a long tail portion was used as electrical lead to the electrodes. The geometric area of both these electrodes was about 0.5 cm^2. A rectangular piece of the foil (25 mm $\times$ 8 mm) was also used in some experiments where higher currents were necessary to obtain prominent CV curves. The RVC electrode was in the shape of a rectangular strip (25 mm $\times$ 5 mm). The geometric area of the electrode, in contact with the electrolyte, was about 2 cm^2. All the electrodes were tightly connected to an aluminium holder/current collector using male–female threadings on the respective parts.

All the bare carbon electrodes were heated to 1023 K, under vacuum, for more than 5 h. In the case of the compacted graphite and glassy carbon electrodes, the bottom surface exposed in the melt was polished thoroughly with 1/0 to 5/0 emery paper. The electrodes, after final assembly, were stored inside an inert atmosphere glove box.

2.2. *Cell*

A Pyrex glass vessel (40 mm ID $\times$ 90 mm long) with a Teflon lid contained the molten electrolyte and electrodes. The electrolyte was prepared by heating a mixture of sodium chloride and aluminium chloride at about 448 K. Sodium chloride (99.9%, Glaxo, India), dried at 723 K under vacuum for more than 12 h and aluminium chloride (99.9%, Fluka, iron free), as received, were used. The brownish looking $NaAlCl_4$ liquid was electrolysed with aluminium electrodes (rod, 3 mm dia., 99.99%, Leiko, USA) at a current density of 1–2 mA cm^{-2}, until the electrolyte liquid looked clear and colourless. Excess NaCl was added to the melt to make it NaCl saturated.

The carbon sample, an aluminium rod (3 mm dia., 99.99%, Leiko, USA) wound spirally for high surface area and a high purity aluminium wire (0.5 mm dia., 99.999%, Aldrich, USA) served as the working, counter and reference electrodes, respectively. The aluminium reference electrode placed in NaCl-saturated $NaAlCl_4$ was physically separated from the rest of the cell by containing it in a glass tube (6 mm dia.), fused at one end, with a small orifice at the fused end. A thick pad of glass wool placed at the fused end prevented the mixing of the reference cell electrolyte with that of the bulk electrolyte. The electrodes and a glass thermowell were introduced to the melt through holes drilled on the Teflon lid of the glass vessel (Figure 1(d)).

The preparation and purification of the reactive electrolyte and the experiments as such were conducted inside an argon atmosphere glove box used for handling liquid sodium metal. The purity of the box atmosphere was better than 2 ppm for air/moisture. The heating of the cell was achieved by a resistance furnace, whose temperature was controlled to within ± 1 °C by a proportional temperature controller (model IT-401-D2, Indotherm, India). The electrolyte temperature was measured using a chromel–alumel thermocouple placed inside the glass thermowell.

2.3. *Measurement techniques and conditions*

The cyclic voltammograms were recorded using a potentiostat/galvanostat (model 173, PAR) coupled to voltage scan generator (EG&G, Universal programmer, model 175). The current and potential signals were recorded using a Data acquisition system (HP 34970A, Data acquisition/switch unit). The data processing was carried out using an IBM compatible computer interfaced to the Data Acquisition System.

The potentials and scan rates used in the CV experiments ranged from $+0.5$ to $+3.0$ V vs Al and 1 to 50 mV s^{-1}. The temperature range of the study was generally 428–523 K, with a few exceptions to a maximum temperature of 573 K. Scan rate of 10 or 20 mV s^{-1} was found suitable for recording the CVs of compacted carbon rods. But, low scan rates in the range 1–10 mV s^{-1} were necessary to obtain the CV of

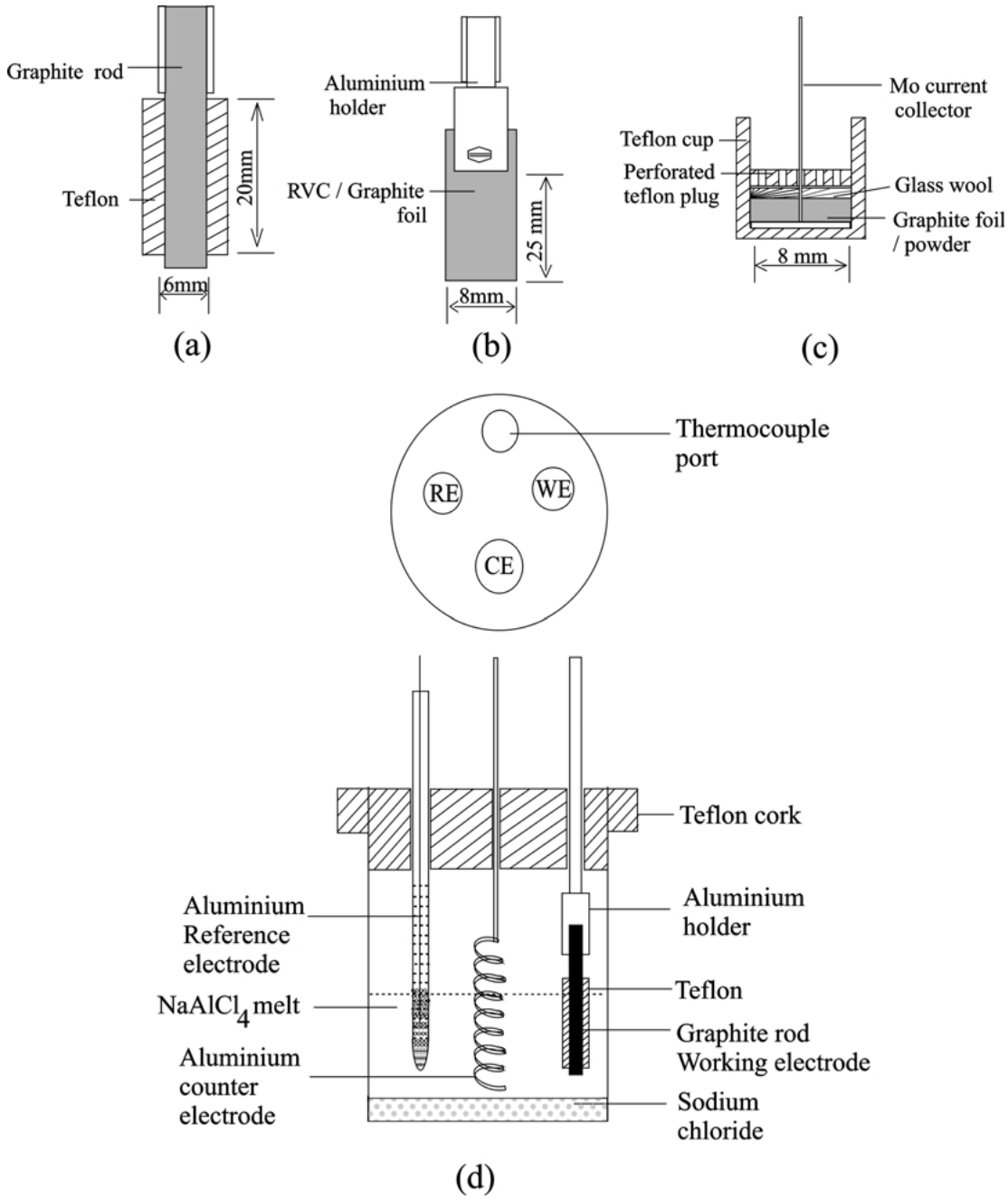

Fig. 1. Fabrication details of the carbon working electrodes: (a) compacted graphite/glassy carbon, (b) RVC/graphite foil, and (c) graphite foil/powder. Schematic of the CV cell is shown in (d).

graphite powders with its characteristic features. At scan rates above 20 mV s^{-1}, the voltammograms looked diffused and featureless.

Fresh electrodes behaved erratically with respect to current during potential cycling. But a few cycles with anodic potentials extending beyond the chlorine evolution potential (2.2 V at 448 K) activated the electrodes. The electrolyte temperature or the duration of stay of the electrode in the fused electrolyte were not very effective in the electrode activation.

Starting at a potential +1 V (or +0.5 V), the parameter was changed in the anodic direction, at a desired scan rate, till the preset anodic potential limit was reached. Then the direction of polarization was reversed until the starting point was reached again.

3. Results and discussion

The cyclic voltammogram of the NaCl saturated electrolyte melt obtained at 458 K, on a tungsten electrode, is given in Figure 2. Two type of anodic chlorine currents, (a) and (b) are shown in the voltammogram. Portion (a) corresponds to the discharge of the dissolved chloride ions in the melt ($2Cl^- \rightarrow Cl_2 + 2e^-$) and (b) is due to the decomposition of the electrolyte

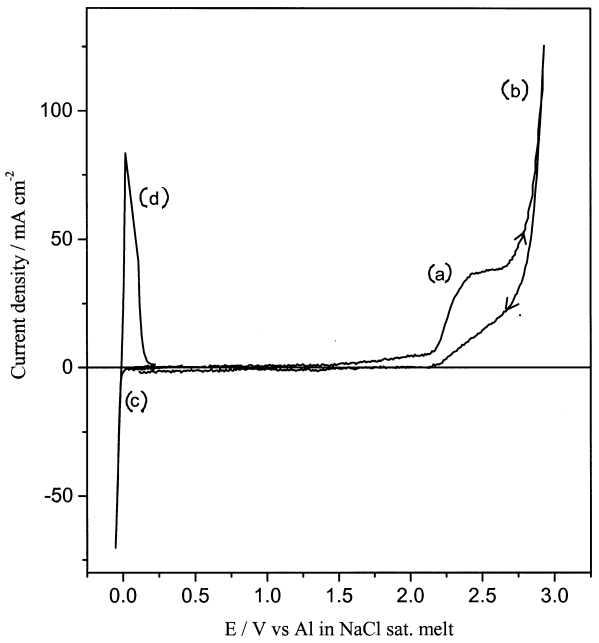

Fig. 2. Cyclic voltammogramme of the NaCl saturated $NaAlCl_4$ melt on W electrode (area 0.008 cm^2) at 458 K. Scan rate 10 mV s^{-1}. (a) and (b) corresponds to the discharge reactions $2Cl^- \rightarrow Cl_2 + 2e^-$ and $4AlCl_4^- \rightarrow 2Al_2Cl_7^- + Cl_2 + 2e^-$, respectively. The cathodic deposition and anodic dissolution of aluminium are shown by (c) and (d). $E_{Cl^-/Cl_2} = 2.197$ V.

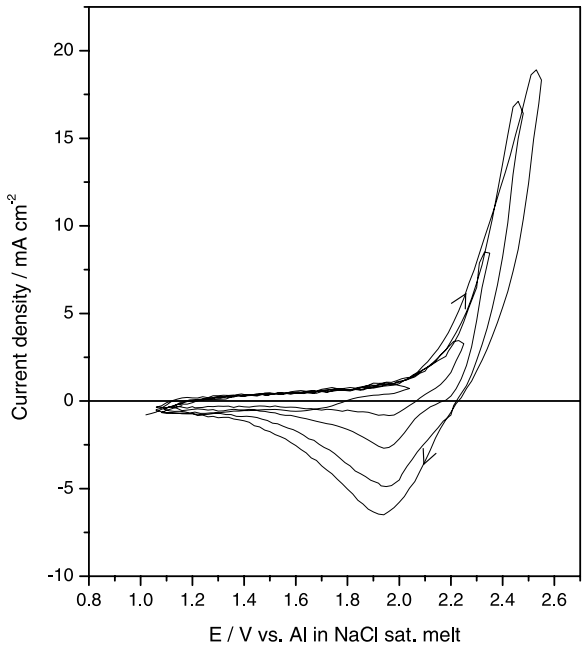

Fig. 3. Cyclic voltammogrammes obtained on fresh graphite rod (surface area 0.5 cm^2) at 448 K. Scan rate 20 mV s^{-1}. Five successive cycles with anodic limit increasing from +2.1 to +2.6 V are combined in the Figure. Increase in the magnitude of the cathodic deintercalation hump with increasing anodic limit shows the direct relationship of chlorine in the intercalation reaction. $E_{Cl^-/Cl_2} = 2.202$ V.

($4AlCl_4^- \rightarrow 2Al_2Cl_7^- + Cl_2 + 2e^-$). The absence of any peaks between the potential window of the electrolyte, that is, aluminium deposition on the cathodic side and chlorine evolution on the anodic side, was taken as an indication that the electrolyte was free of impurities. It can be seen from the voltammogram that chlorine evolves on the anode at potentials positive to +2.2 V vs Al. The Chlorine equilibrium potentials in the melt are important in the present context, as these have a direct bearing on the anodic behaviour of the carbon electrodes discussed below. Our measurements [10] show that the Cl^-/Cl_2 equilibrium potentials fall in the range 2.210–2.137 V in the temperature range (433–573 K) of this study.

3.1. *Effect of carbon materials*

Preliminary cyclic voltammetric studies on different types of carbonaceous materials in chloroaluminate melt showed three distinctly identifiable voltammetric patterns during the initial period of cycling.

3.1.1. *Compacted graphite*

Typical cyclic voltammetric responses of a fresh graphite rod electrode in the basic sodium chloroaluminate melt at 448 K are given in Figure 3. Five cyclic voltammograms with anodic potential limits increasing by 0.1 V in the successive runs, in the potential window from +2.0 to +2.5 V, are combined in the Figure. The CV shows no significant negative current until the potential is 2.2 V. For potentials above 2.1 V, the graphite electrode shows current in the reverse (cathodic) scan in sharp contrast to the behaviour on the W electrode (Figure 2). As the anodic potentials were made more and more positive, the cathodic currents showed a corresponding increase. This observation makes it apparent that the graphite reacted anodically in the melt in presence of chlorine and the reaction products were discharged in the reverse scan to give rise to the cathodic current. As graphite does not form stable chlorides with chlorine above 273 K [11], the reversible anodic reaction products can be reasonably confirmed as graphite intercalation compounds involving $AlCl_3$ and chlorine, as reported by Wendt et al. [4]. Chemical characterization of these compounds could not be carried out as the excess electrolyte present on the samples interfered with the analysis. Attempts to remove the excess electrolyte destroyed the sample itself. However, SEM pictures of the washed graphite sample recovered from the sodium production cell, showed exfoliation and swelling of the electrode (Figure 4). It is well known that the graphite crystal lattice expands along the *c*-axis during intercalation. The volume expansion of the electrode probably resulted in its eventual disintegration.

The present results can be compared with the vapour phase intercalation of aluminium chloride in graphite in the presence of chlorine [12–22]. Rudorff [12] reported that gaseous chlorine is a prerequisite for the intercalation of aluminium chloride in graphite. Dzurus and Henning [13] reconfirmed the findings of Rudorff and showed that the intercalation reaction ceased when the chlorine in the reaction mixture was exhausted.

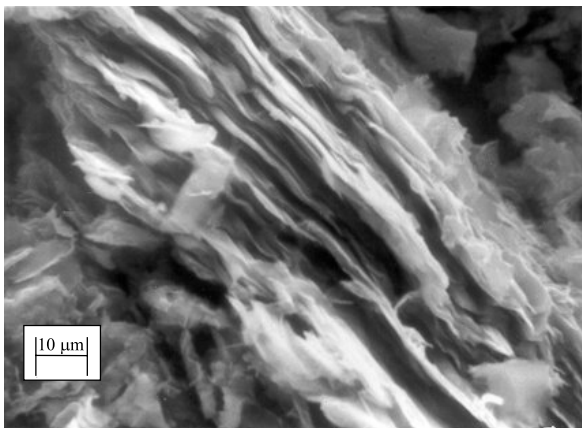

Fig. 4. The scanning electron micrograph of a sample of the reacted graphite anode recovered from the low-temperature sodium production cell, graphite/NaCl, $NaAlCl_4$/β-alumina/Na. The graphite anode was used in the cell operating at 498 K at 10 mA cm^{-2} for $\sim$ 100 h. The SEM picture shows that the graphite is exfoliated as a result of the intercalation reaction.

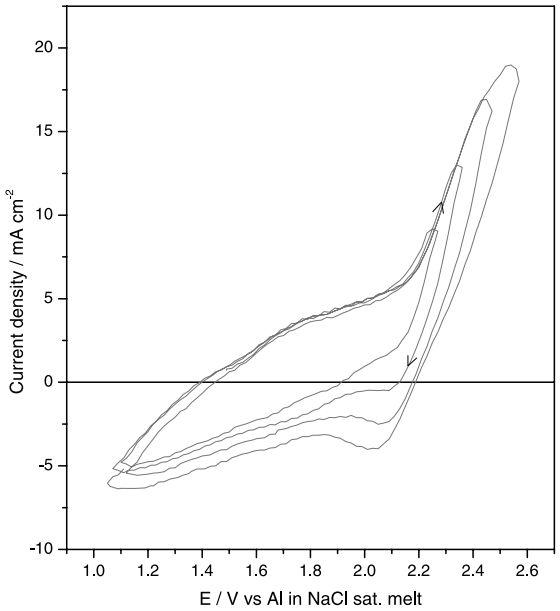

Fig. 5. CV responses of the graphite foil (disc surface area 0.5 cm^2) electrode at 448 K. Scan rate 20 mV s^{-1}. Four successive cycles with anodic limits increasing from 2.1–2.5 V are shown in the Figure. The CV shows the increase of current in the subchlorine evolution potential as a result of adsorption of chloride ions. The magnitude of the chlorine-induced intercalation/deintercalation processes is less on the electrode in comparison to the compacted graphite rod electrode. $E_{Cl^-/Cl_2} = 2.202$ V.

Graphite Intercalation Compounds (GIC) with varying composition of carbon, aluminium chloride and chlorine are reported in these studies. Different formulae, such as $C^+AlCl_4^- \cdot xAlCl_3$ [12], $C_n^+Cl^- \cdot 3AlCl_3$ [13] and $C_{18}^+AlCl_4^-AlCl_3$ [14] have been proposed by independent investigators. Our analysis of the GIC, based on the galvanostatic measurements [8], indicated that the empirical formula is $C_n^+Cl^- \cdot AlCl_3$ or $C_n^+AlCl_4^-AlCl_3$.

3.1.2. *Graphite foil*

Typical cyclic voltammograms obtained at 448 K, with anodic potential limits increasing in the successive runs, on a fresh graphite foil electrode are presented in Figure 5. As in the case of the rod electrode, the negative hump due to deintercalation is seen for cycles with anodic potential above 2.2 V. But, even though the experimental conditions remain more or less the same, the background current in the region below 2.0 V on the electrode is substantially higher than that obtained on the compacted rod (compare Figures 3 and 5). This background current, also increases with increase in electrode potential. Due to this, the shape of the CV curves of the two electrodes looks distinctly different. The voltammetric behaviour may be explained by the porosity-dependant surface area of the electrodes, as discussed in the following section.

3.1.3. *Graphite powder*

A typical cyclic voltammogram obtained on fresh graphite powder electrode at 428 K with anodic potential 2.3 V and scan rate 1 mV s^{-1} is shown in Figure 6. Two distinct types of voltammetric behaviour can be observed. Unlike the case of the graphite rod electrode, a well-defined anodic/cathodic redox couple (1,2) is seen in the potential region below chlorine evolution, in addition to the characteristic intercalation/deintercalation peaks (3,4). The anodic chlorine current (3) is seen to start at a slightly lower potential than the chlorine equilibrium potential. Though a straightforward explanation of this behaviour is difficult, it seems that the reaction of chlorine on the high surface area and active carbon sites contributes to it.

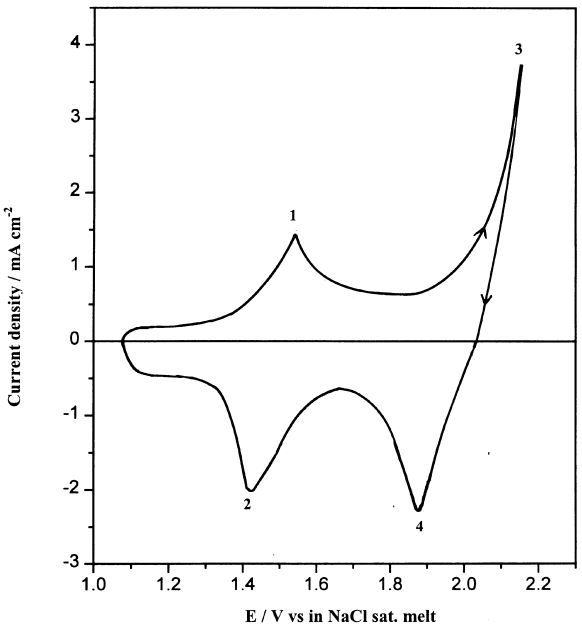

Fig. 6. CV response of the graphite powder electrode (surface area 0.5 cm^2) at 428 K. Scan rate 1 mV s^{-1}. The adsorption/desorption (1,2) and intercalation/deintercalation (3,4) peaks are distinctly seen in the Figure. $E_{Cl^-/Cl_2} = 2.212$ V.

Table 1. Effects of scan rate on the redox process on graphite powder electrode below chlorine evolution potential. Anodic potential limit 1.9 V, temperature 473 K

S. no	Scan rate/mV s^{-1}	Peak potential/V		Peak current/mA	
		Anodic $E_{p,a}$	Cathodic $E_{p,c}$	Anodic $i_{p,a}$	Cathodic $i_{p,c}$
1	1	1.551	1.470	0.18	0.14
2	2	1.563	1.456	0.28	0.29
3	5	1.590	1.434	0.62	0.59
4	10	1.656	1.364	1.10	0.99
5	20	1.712	1.281	1.50	1.89

To obtain more information on the anodic/cathodic processes below chlorine evolution, CV curves were recorded at different scan rates from 1–20 mV s^{-1} at a fixed anodic potential limit of +1.9 V. The peak separation ($\Delta E_p = E_{p,a} - E_{p,c}$) at slow sweep rates can be as low as 80 mV as shown in Table 1. The anodic and cathodic peak currents are also close to each other. The current values obtained are only a few mA cm^{-2}, which is substantially lower than the currents involved in the intercalation/deintercalation processes. These observations showed that the redox couple corresponds to a quasi-reversible process and the process is substantially different from the chlorine-assisted chlorolauminate intercalation/deintercalation process discussed above. The logarithm of the peak currents of the anodic ($i_{p,a}$) and cathodic ($i_{p,c}$) processes when plotted against the logarithm of scan rate (v) resulted in straight lines with slopes, 0.74 and 0.84, respectively. This indicates that the redox process is predominantly due to adsorption/desorption [23] taking place on the fine graphite powder particles. Compared to the compacted graphite material, graphite powder has a higher concentration of exposed grain boundaries, edge sites and other defects. Adsorption of loosely held chlorine free radicals at such active sites may be responsible for the redox process in the potential region

$$C_x + Cl^- \Leftrightarrow C_x\text{—}Cl + e^-$$

Similar observations were made in our galvanostatic experiments [8] with a graphite powder electrode. In these experiments, the anodic currents were noticed from 1.4 V onwards.

The three graphite electrodes, viz. compacted rod, foil and powder, are compared, under identical experimental conditions, in Figure 7. The currents, at potentials below chlorine evolution, can be seen increasing in the order rod < foil < powder. The porosity of the electrodes also increases in the same order. Also, the shape of the voltammograms changes as the electrode porosity is increased. While chlorine evolution at 2.2 V is distinctly clear on the rod electrode, it is almost indistinguishable on the powder electrode. This shows that the chlorine evolution is suppressed on a high-surface carbon anode and the chloride ions predominantly adsorb on the active carbon sites. The results make it clear that the effective surface area of the three electrodes are different, owing to their different degrees of porosity, even though their geometric area was more or less the same (0.5 cm^2).

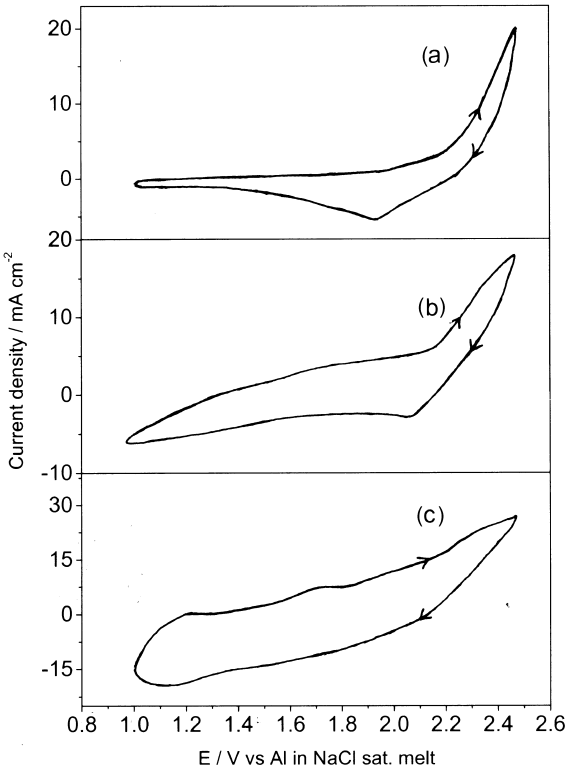

Fig. 7. CV curves obtained on (a) graphite rod (b) graphite foil and (c) graphite powder electrodes under identical experimental conditions. Temperature 448 K. Scan rate 20 mV s^{-1}. Anodic limit 2.5 V. The change of the electrode processes from chlorine evolution (intercalation)/deintercalation to surface adsorption/desorption with increasing porosity of the electrode is visible in the voltammograms.

3.1.4. *Glassy carbon and RVC*

A typical CV of glassy carbon electrode (GCE) in basic chloroaluminate melt at a sweep rate of 10 mV s^{-1} is presented in Figure 8. The voltammetric response is similar to that on the inert W electrode (Figure 2). Significant anodic current is noticed only beyond 2.1 V. No cathodic current is noticed on both these electrodes during the reverse sweep within the potential limit. These observations suggest that the electrochemical processes taking place on GC is similar to those occurring on the W electrode under identical conditions.

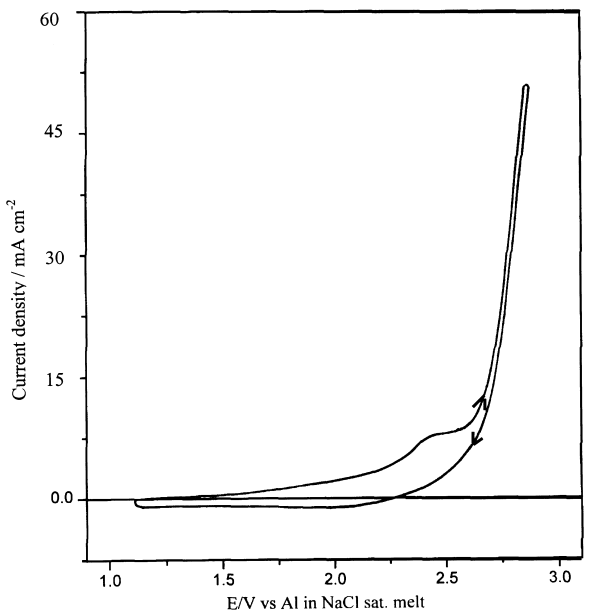

Fig. 8. Cyclic voltammogram on the GC electrode (2 mm dia., 0.03 cm^2) at 458 K. Scan rate 10 mV s^{-1}. Absence of the cathodic deintercalation current shows the inertness of the electrode to chlorine. $E_{Cl^-/Cl_2} = 2.197$ V.

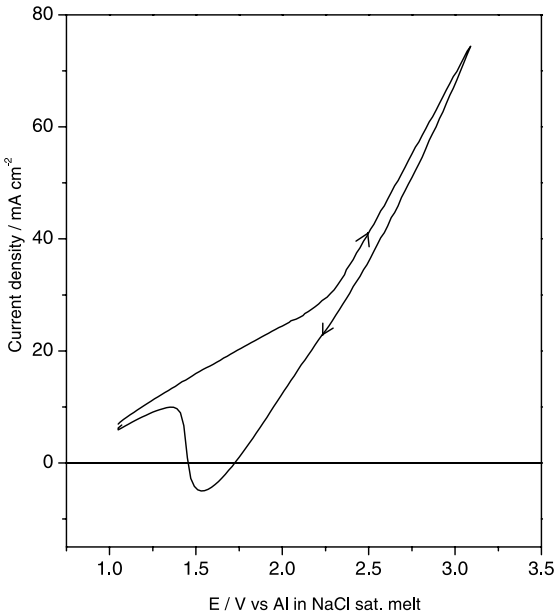

Fig. 9. CV curve obtained on the RVC (surface area 2 cm^2) at 448 K. Scan rate 20 mV s^{-1}. The electrode was polarized a few times with anodic potentials above +2.5 V before recording the CV. $E_{Cl^-/Cl_2} = 2.202$ V.

Hence the chlorine-evolving GC anode, unlike graphite, is inert in the chloroaluminate melt.

A fresh RVC electrode was polarized under the same experimental condition as those of the GC electrode. In spite of polarising to +3.0 V, no negative currents were noticed in the CV. However, after many charge-discharge cycles with an anodic limit of +2.5 V, the electrode showed negative currents in the reverse sweep (Figure 9) indicative of intercalation/deintercalation reactions. Such an effect was not observed in the case of the GC electrode.

It has been reported that highly crystalline carbon (graphite) is a prerequisite for reversible intercalation of suitable anions. Carbon of low crystallinity exhibits no intercalation [24]. GC and RVC are predominantly amorphous carbon materials with small concentration of islands of graphitic layers. The amorphous nature of these electrodes may be the reason for the poor intercalation efficiency. As the electrodes are subjected to repeated cycling, more and more graphitic regions may become exposed to the melt for intercalation and hence show a pattern of intercalation as shown in the case of the cycled RVC electrode (Figure 9). Obviously, for this to happen, the carbon electrode should have better porosity and high surface area. However, by virtue of the method of production [25], GC is compact with closed pores and hence proper orientation of ionic species for insertion and exfoliation of the solid phase during intercalation are not possible. From a practical point of view, such electrode materials would be the ideal chlorine-evolving anodes in the chloroaluminate melts.

The voltammogram shown in Figure 9 shows significant current in the subchlorine evolution potentials. As is the case of the powder and foil electrodes, these currents are possibly related to the surface adsorption of anionic species in the melt. The entangled mesh-type structure of the carbon threads in RVC with a void volume of 90 to 97% [25] gives very high porosity to the carbon material. The feasibility of a secondary battery based on the adsorption/desorption of chloride ions on high surface carbon, as patented by Werth [26], is evident from these results.

3.2. *Parameters affecting the electrode behaviour*

Under the present experimental conditions, chlorine evolution and chlorine-assisted intercalation are competitive anodic processes. The term current efficiency (c.e) or intercalation–deintercalation efficiency (IDE) is given by

$$\text{IDE} = \text{c.e} = Q_\text{d}/Q_\text{c}$$

where Q_d and Q_c are the discharge and charge capacities, respectively. This is used in the following Sections to present a semiquantitative analysis of the redox process. The parameters controlling the current efficiency are found to be anodic potential, temperature, scan rate and cycling and porosity.

3.2.1. *Anodic potential*

The effects of anodic potential on the intercalation and deintercalation charges and IDE on a compacted graphite electrode at 444 K are presented in Table 2. Both anodic and cathodic processes are favoured at higher oxidation potentials. However, the efficiency of the intercalation process increases to a maximum of

Table 2. Variation of anodic and cathodic charges and IDE with anodic potential limit evaluated using the CV response of a compacted graphite electrode. Temperature 435 K, scan rate 20 mV s^{-1}

Anodic limit/V	Charge/C		IDE Q_d/Q_c
	Anodic/Q_c	Cathodic/Q_d	
2.17	0.026	–	–
2.27	0.056	0.015	0.266
2.34	0.109	0.042	0.388
2.48	0.229	0.129	0.563
2.56	0.364	0.212	0.582
2.67	0.607	0.308	0.508
2.76	0.849	0.406	0.479
2.88	1.202	0.491	0.408
2.98	1.56	0.642	0.411

about 50% at 2.5 V and then falls. This means that at anodic potentials above 2.5 V, chlorine gas evolution on the graphite electrode dominates the intercalation reaction. At higher anodic potentials, when the rate of generation of chlorine is much greater, the intercalation or ionic insertion rate into the graphite lattice becomes comparatively smaller and free Cl_2 gas escapes rather than assisting intercalation.

As the anodic potentials are made more and more positive, the cathodic charge, as well as the potential window of the charge, expand (Figure 3). The slowness of the discharge process with increasing depth of intercalation and/or the dependence of chlorine activities in the intercalation compounds are probable reasons for such behaviour. Intercalation compounds with a wide range of chlorine activities are possible depending on the extent of chlorine available at the anode. The observation is in line with results of vapour phase experiments of Dzurus and Henning [13].

3.2.2. *Temperature*

The effect of temperature on all the carbon electrodes studied was similar; the higher the temperature the lower the deintercalation charge, and hence the IDE. This aspect of the electrode behaviour, with compacted graphite rod as an example, can be seen from the data presented in Table 3. The lowering of the cathodic charge, and hence the IDE, with increase in temperature shows that the anodic process is predominantly chlorine evolution at higher temperatures. At higher temperatures, the electrochemically generated chlorine gas escapes from the electrode surface rather than assisting intercalation. Consequently the attack and disintegration of the carbon anode is less severe at high temperatures. A cut off temperature beyond which the intercalation reaction will not be feasible cannot be obtained from the limited temperature (573 K maximum) of the present study. However, from the observation of Wendt et al. [4] that the carbon anodes are virtually stable above 873 K, even in acidic chloroaluminate melts, suggests that the operation temperature in the noncorrosive, basic chloroaluminate melt is well below 873 K.

The implications of the temperature dependence of the graphite intercalation reactions are two-fold: (i) for better stability of the graphite anode and higher chlorine efficiency, electrolysis of molten chloroaluminate needs to be carried out at higher temperatures (>700 K) (ii) A low operation temperature (<500 K) is ideal for a secondary battery which uses the intercalation compounds as positive electrode.

At temperatures close to the electrolyte melting point (424 K), the cathodic deintercalation peaks split into two or three. However such splitting is not observed at higher temperatures. It seems that the distinguishable energy states for different stages of intercalation can be observed at lower temperatures only. Similarly the characteristic current peaks corresponding to the adsorption/desorption as well as the intercalation/deintercalation processes on the graphite powder electrode (Figure 6) were clearly distinguishable at low temperatures only. As temperature increased, these fine features appeared increasingly diffused.

3.2.3. *Scan rate*

The charge–discharge behaviour of all the compact carbon electrodes with scan rate was similar. The Q_c and Q_d and IDE values obtained for typical CV curves of a rod electrode at different sweep rates of 5, 10, 20 and

Table 3. Variation of anodic and cathodic charges and IDE with temperature evaluated using the CV responses of a graphite rod electrode. Scan rate 20 mV s^{-1}, anodic limit 2.5 V

Temperature/K	Charge/C		IDE Q_d/Q_c
	Anodic/Q_c	Cathodic/Q_d	
435	0.203	0.151	0.598
451	0.292	0.132	0.453
470	0.363	0.112	0.308
486	0.423	0.085	0.203
504	0.522	0.079	0.151
516	0.585	0.059	0.101
538	0.68	0.05	0.073
552	0.725	0.041	0.056
573	0.773	0.025	0.033

Table 4. Variation of anodic and cathodic charges and IDE with scan rate evaluated using the CV responses of a graphite rod electrode. Temperature 448 K, anodic limit 2.5 V

Scan rate/mV s^{-1}	Charge/C		IDE Q_d/Q_c
	Anodic/Q_c	Cathodic/Q_d	
5	7.02	2.24	0.319
10	4.45	1.81	0.406
20	2.21	1.44	0.651
50	1.07	0.932	0.871

50 mV s^{-1} are given in Table 4. As expected, both the anodic and cathodic charges decrease with scan rate, but the increase in the intercalation efficiency with scan rate is significant. This consistent observation suggests that, of the two competitive anodic reactions (viz., chlorine evolution and intercalation) the intercalation reaction is favoured at high scan rates. This contradicts the usual experimental observation that the intercalation reaction is slow. From the apparently conflicting results, it may turn out that the charge transfer reaction taking place on surface layers close to the edges of the graphite layer is indeed very fast [25], but the slow diffusion of the intercalates into the bulk limits further reaction, thus making it appear that the intercalation reaction is slow.

The combined effect of temperature and anodic limit on IDE is shown in Figure 10.

3.2.4. *Cycling and porosity*

The CV responses of the graphite powder electrode before and after cycling are shown in Figure 11. The anodic potential limit was maintained at +2.5 V during the charge/discharge cycles. The current is greater after cycling. Also, the cycling changes the shape of the voltammogram. The results of the particle size analysis of the graphite powders, given in Figure 12, also show that the particle sizes have increased due to cycling.

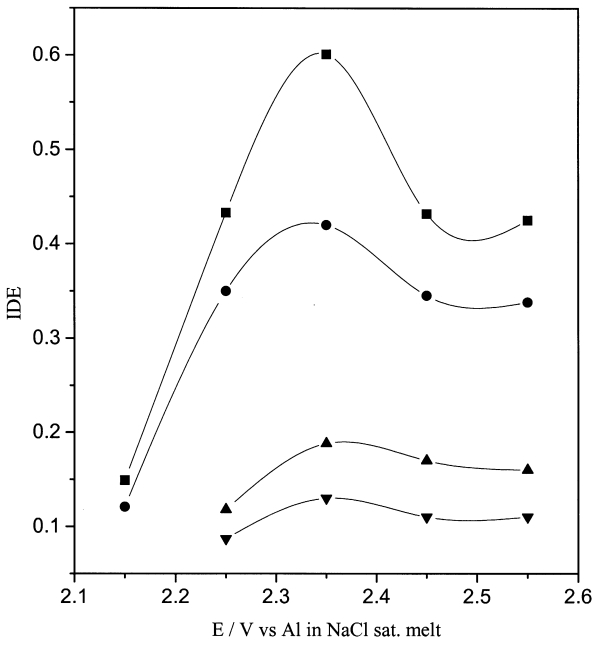

Fig. 10. Variation of the intercalation/deintercalation efficiency of a graphite rod electrode with temperature and anodic potential. Scan rate 20 mV s^{-1}. Key: (■) 448, (●) 483, (▲) 513 and (▼) 538 K.

Intercalation is accompanied by swelling of the graphite crystal along the *c*-axis. During the deintercalation process, the crystal shrinks with microcracks developing on the surface. The effective surface area of the electrode, therefore, increases substantially with repeated charge/discharge cycles [27] as revealed in the particle size analysis. Janssen [28, 29] showed that chlorine evolution on graphite during electrolysis of acidic, aqueous NaCl takes place in two steps, i.e. by charge transfer $Cl^- \rightarrow Cl_{ads} + e^-$ and electrochemical desorption, $Cl_{ads} + Cl^- \rightarrow Cl_2 + e^-$ and both the steps are simultaneously rate determining at a fresh electrode surface. At an aged or modified graphite anode, the electrochemical desorption step becomes rate controlling. Thus, the higher currents observed on cycled electrodes below the chlorine evolution potential, in the present case, may also be attributed to the surface adsorption of chloride ions on the enlarged surface area of the powders. The difference in the current–potential characteristics on the modified electrode surface is manifested in the shape of the voltammogram.

The results show that the graphite electrodes, on repeated cycling, lost their ability for chlorine evolution and the electrode surface changed to an ionic salt layer. The speed and magnitude of these transformations depend on the number of charge/discharge cycles, the anodic potential limit, temperature and the physical nature of the graphite electrodes. The ease of transformation was found to increase in the order rod < foil < powder. The fact that the porosity of the electrodes also increased in the same order showed that the intercalation related surface deteriorations are possibly related to the particle size of the electrode. These aspects of the anodic processes are still under investigation.

4. Conclusion

The CV studies have revealed that carbon anodes, in the time scale of this study, are inert in the basic sodium chloroaluminate melt below the chlorine evolution potential. Chlorine evolving graphite anodes react in the melt to form reversible graphite intercalation compounds, which affect the stability as well as the chlorine efficiency of the electrode. The magnitude of the

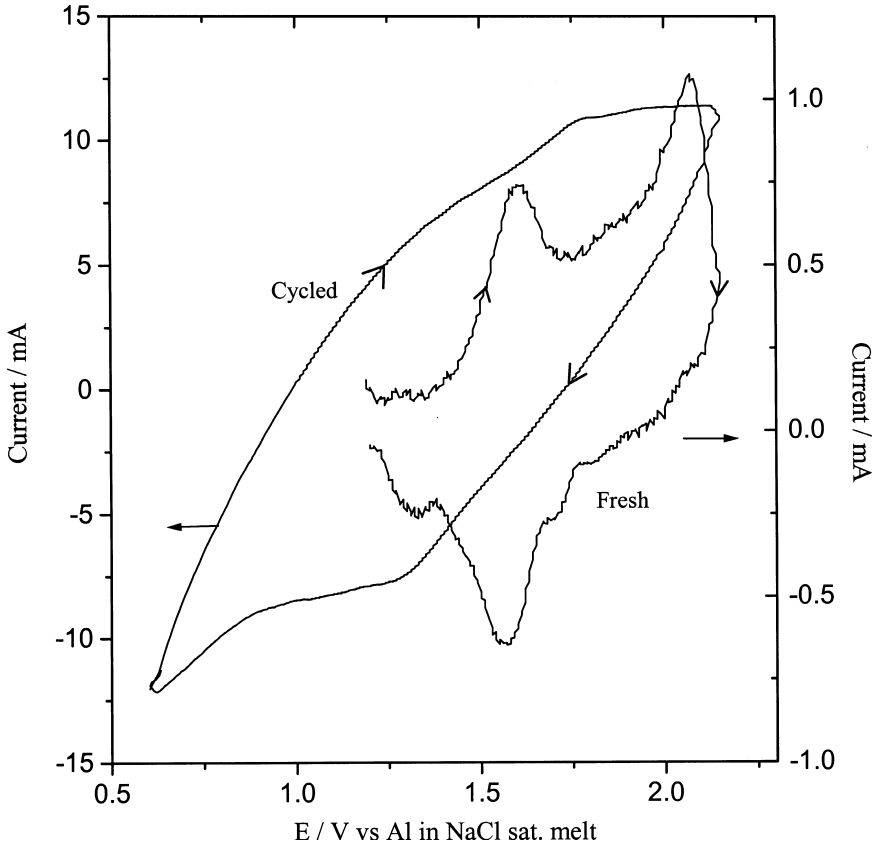

Fig. 11. Cyclic voltammograms of the graphite powder electrode recorded while fresh and after cycling 25 times with anodic limit +2.5 V. Scan rate 5 mV s^{-1}. Temperature 438 K. The cycled electrode shows significant increase in current, suggesting of the increase in surface area due to the intercalation/deintercalation processes. Due to surface transformation, the fine voltammetric features of the fresh graphite electrode is not seen after cycling.

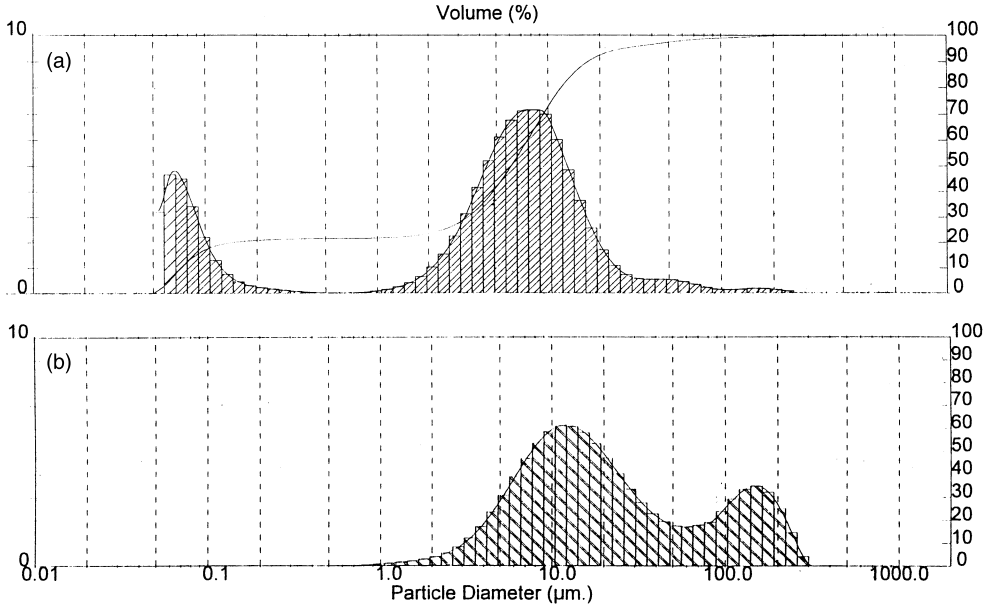

Fig. 12. The particle size distribution of the (a) fresh and (b) cycled graphite powder electrode obtained by light scattering method (Malvern zeta sizer-3). The average size of the powder particles has increased on cycling.

intercalation reaction is directly related to the extent of chlorine available on the anode. The study confirms the role of chlorine as one of the reactants in the intercalation of $AlCl_3/AlCl_4^-$ in graphite by an electrochemical technique. Predominantly amorphous carbons like glassy carbon do not show much reactivity towards

chlorine and hence is a better anode material for low-temperature electrolysis of molten chloroaluminate.

Intercalation reactions are less favoured at higher temperatures and hence the stability and chlorine efficiency of a graphite anode improve with increase in temperature. For the same reason, a secondary battery using the GIC as positive electrode will be less efficient at higher temperatures. Substantial quantities of chloride ions can be reversibly adsorbed on high surface carbon at potentials below chlorine evolution and hence it can be used as a positive chlorine electrode, which does not require handling of chlorine gas or anodic generation of chlorine. The possibility of a secondary sodium–chlorine battery using both intercalation/deintercalation and adsorption/desorption processes combined can be inferred. However, such a system may not be feasible due to deterioration of the carbon electrode with cycling.

References

1. *British Patent, 1 200 103* (1967).
2. Yashuhiko Ito and Shiro Yoshizawa, Some new molten salt electrolytic processes, *in* G. Mamantov and J. Braunstein (Eds), 'Advances in Molten Salt Chemistry', (Plenum, New York, 1981), p.391.
3. K.S. Mohandas, N. Sanil and P. Rodriguez, Proceedings of the National Symposium on Electrochemistry in Nuclear Technology (Kalpakkam, 1998), pp. 163–168.
4. H. Wendt, A. Khalil and C.E. Padberg, *J. Appl. Electrochem.* **21** (1991) 929.
5. G.L. Holleck, *J. Electrochem. Soc.* **119** (1972) 1158.
6. A.J. Bard, 'Encyclopedia of Electrochemistry of the Elements' (Marcel Dekker, Inc., New York, 1976) vol. X, p. 263.
7. H. Wendt, S. Dermeik and A. Ziogas, *Werkst Korros.* **41** (1990) 457–463.
8. K.S. Mohandas, PhD thesis, University of Madras, January (2001).
9. S. Maximovitch, M. Levart, M. Fouletier, N. Nguyen and G. Bronoel, *J. Power Sources* **3** (1978) 215–225.
10. K.S. Mohandas, N. Sanil, Tom Mathews and P. Rodriguez, *Metall. Mater. Trans. B*, in press.
11. W. Rudorff, *in* 'Advances in Inorganic Chemistry and Radiochemistry' vol. 1, (1959), p. 254.
12. W. Rudorff and A. Landel, *Z. Anorg. Allg. Chem.* **293** (1958) 327.
13. M.L. Dzurus and G.R. Henning, *J. Amer. Chem. Soc.* **79** (1957) 1051.
14. B. Bach and A.R. Ubbelhode, *Proc. R. Soc. Lond. A* **325** (1971) 437.
15. J.G. Hooley, *Carbon* **11** (1973) 225.
16. R.C. Croft, *J. Appl. Chem.* (Lond.) **2** (1952) 557.
17. J.G. Hooley and P.T. Hough, *Carbon* **16** (1978) 221.
18. Baikar, E. Habegger, V.K. Sharma and W. Richard, *Carbon* **19** (1981) 329.
19. Baikar, E. Habegger and R. Schlogl, *Ber. Bunsenges. Phys. Chem.* **89** (1985) 530.
20. M. Fouletier and M. Armand, *Carbon* **17** (1979) 427.
21. J.G. Hooley, *Carbon* **18** (1980) 83.
22. E. Stumpp, *Mater. Sci. Eng.* **31** (1977) 53.
23. D.K. Gosser, Jr, 'Cyclic Voltammetry – Simulation and Analysis of Reaction Mechanisms' (VCH, New York, 1996), p. 43.
24. H. Thiele, *Z. Electrochem.* **40** (1934) 26.
25. K. Kinoshita, 'Carbon: Electrochemical and Physiochemical Properties' (J. Wiley & Sons, New York, 1988).
26. J.J. Werth, *US Patent 3 847 667* (1974).
27. P. Beck, H. Junge and H. Krohn, *Electrochim. Acta* **26** (1981) 799.
28. L.J.J. Janssen and J.G. Hoogland, *Electrochim. Acta* **15** (1970) 941.
29. L.J.J. Janssen, *Electrochim. Acta* **19** (1974) 257.